

Towards T_1 -limited magnetic resonance imaging using Rabi beats

H. Fedder,^{1,*} F. Dolde,¹ F. Rempp,¹ T. Wolf,¹ P. Hemmer,² F. Jelezko,¹ and J. Wrachtrup¹

¹*3rd Physics Institute and Research Center SCoPE,
University of Stuttgart, Pfaffenwaldring 57, 70550 Stuttgart*

²*Department of Electrical and Computer Engineering,
Texas A&M University, College Station, TX 77843, USA*

(Dated: 2010-09-03)

Two proof-of-principle experiments towards T_1 -limited magnetic resonance imaging with NV centers in diamond are demonstrated. First, a large number of Rabi oscillations is measured and it is demonstrated that the hyperfine interaction due to the NV's ^{14}N can be extracted from the beating oscillations. Second, the Rabi beats under V-type microwave excitation of the three hyperfine manifolds is studied experimentally and described theoretically.

INTRODUCTION

The ever increasing need for high resolution imaging in the life sciences, material science, and more recently quantum information processing, has led over the past decade to the development of a variety of methods that try to overcome the limits set by optical diffraction [11]. Exploiting the non-linear behaviour of fluorescent labels, a spatial resolution down to few nanometers was demonstrated using optical techniques such as STED [6], PALM [3], and STORM [13]. A technique whose resolution is independent of the wavelength, is magnetic resonance imaging. Magnetic resonance imaging – and nano scale magnetic- and electric field sensing – are key technologies in various areas of science. Recently, magnetic resonance imaging as well as scanning probe magnetic imaging on scales relevant to molecular biological processes was demonstrated [1, 8]. A spin label that is suitable for high resolution measurements are nitrogen vacancy centers embedded in diamond nano crystals [17]. Owing to their optical adressability, photostability and long spin coherence time recently sub 10nm spatial resolution as well as the detection of magnetic fields close to individual electron spins has been demonstrated using NV nano sensors [1, 8]. The spatial resolution of a magnetic resonance measurement is determined by the strength of the field gradient and the effective linewidth of the electron spin transition. Pulsed imaging modes, such as the Hahn-Echo and CPMG sequence can be used to decrease the effective linewidth. The continuous driving of Rabi oscillations has been proposed to decrease the effective linewidth down to the limit given by the spin decay time [16]. In this paper we perform a proof-of-principle study of this imaging mode. The feasibility of the method is demonstrated by resolving the hyperfine interaction of the NV center due to its ^{14}N nuclear spin.

In the simplest magnetic resonance imaging mode, a CW electron spin resonance (ESR) measurement is performed, and the effective linewidth is given by the spin dephasing time T_2^* , which is typically short and only of the order of few micro seconds in case of the NV center.

In the Hahn-Echo sequence, $\pi/2 - \pi - \pi/2$ pulses are used to refocus precessing spins, such that noise generated by slowly fluctuating spins in the environment is canceled. For the Hahn-Echo sequence, the effective linewidth is given by the dephasing time T_2 of the spin system, which is larger than T_2^* , and can reach several hundred microseconds in the case of the NV center [2]. More advanced pulse sequences, such as the CPMG sequence [9], hold promise to decrease the effective linewidth down to the limit set by T_1^ρ [5, 14]. Another elegant imaging mode is based on the continuous driving of Rabi oscillations. The decay time of Rabi oscillations is given precisely by T_1^ρ and depends on the microwave power. When the microwave power is high and the Rabi frequency approaches the transition frequency – corresponding to the limit of the rotating wave approximation – T_1^ρ approaches T_1 . Among the various magnetic resonance imaging modes, this mode may potentially achieve the longest decay time and highest resolution. Over the past years there has been a continued effort to apply this magnetic resonance imaging mode to the NV center [16]. However, this poses great challenges. In this mode, spatial information is extracted from beat frequencies observed in the Rabi oscillations. A high spatial resolution requires the measurement of a large number of Rabi oscillations. Here we demonstrate the feasibility of this imaging mode by realising the measurement of a large number (> 500) of Rabi oscillations, and resolve the hyperfine splitting due to the NV's ^{14}N nuclear spin from the Rabi beats. Moreover, we investigate experimentally and describe theoretically the observed Rabi beats in case of a V-type energy level scheme, which is the desired excitation mode in a high resolution experiment.

The principle of magnetic resonance imaging using Rabi beats is illustrated in Fig. 1. We envision a sample, such as a living cell, that is tagged with nano diamonds that contain single NV-centers. The NV electron spins are initialized and read out optically using a confocal microscope. An inhomogeneous microwave field – such as the one generated by a coplanar waveguide – is applied to the sample. The microwaves are matched to the $m_s = 0 \rightarrow \pm 1$ electron spin transition and drive Rabi

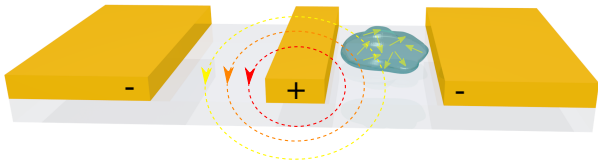


FIG. 1. Principle of magnetic resonance imaging based on Rabi beats.

oscillations between the groundstate spin sublevels. The Rabi frequency depends on the microwave power, thus encoding the position and angle within the microwave field. From an a priori knowledge of the microwave field (or from a reference measurement), the position and angle of the individual NV-centers with respect to the electrodes can be determined. To obtain the NV position in two spatial directions, two successive measurements are performed with microwave gradients applied in different directions using a two dimensional waveguide structure.

In this magnetic resonance imaging mode, the resolution is given by the decay time T_1^p of the Rabi oscillations, the Rabi frequency Ω , and the strength of the microwave gradient. The number N of observable Rabi oscillations is linked to T_1^p and the Rabi frequency as

$$\frac{\Omega T_1^p}{2\pi} = N, \quad (1)$$

For the present coplanar waveguide, the field gradient is determined by the width G of the gap, and the resolution δx follows approximately as

$$\delta x = \frac{G}{N}. \quad (2)$$

The maximum achievable Rabi frequency is of the order of the Lamor frequency of the spin [4]. In this case, the decay time T_1^p of the Rabi signal becomes T_1 and the resolution approaches

$$\delta x = \frac{2\pi G}{T_1 \Omega}, \quad (3)$$

where $\Omega = \omega = D \approx 2.88\text{GHz}$ is equal to the electron spin transition. For NV centers, the T_1 time is typically few ms at room temperature [12], such that a ratio $T_1/\omega = 10^{-6}$ could in principle be achievable. With $G = 10\mu\text{m}$ a spatial resolution of 0.01nm would be reached. However, this poses stringent requirements on the stability of the applied microwave field. Both the power stability and the spatial stability of the microwave field must be at least as good as the ratio T_1^p/Ω , and to achieve sub Angstrom resolution, the microwave wire should not drift by more than a fraction of an atomic diameter.

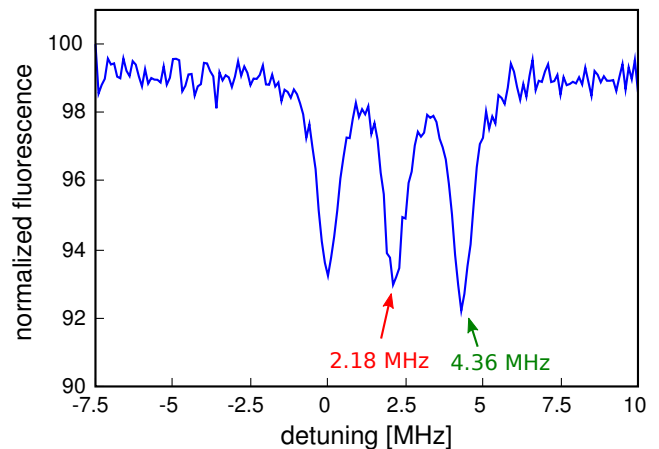


FIG. 2. ESR spectrum of the NV center showing the hyperfine splitting of the $m_s = 0 \rightarrow -1$ spin level due to ^{14}N . The spectrum was recorded with an applied DC magnetic field of about 150G. Detuning is denoted relative to the lowest hyperfine transition corresponding to 2.4524GHz.

RESULTS AND DISCUSSION

To demonstrate the observation of Rabi beats, we study a single NV-center in a fixed microwave field. Rabi beat measurements with a single NV center are possible owing to hyperfine interaction with the NV's ^{14}N nuclear spin, that results in a splitting of the groundstate spin manifold into several hyperfine sublevels. Each hyperfine transition has a slightly different Rabi frequency, which results in a beat signal in the measured Rabi oscillations. These hyperfine beats will also be seen in high resolution Rabi beat imaging data as a modulation, and it is important to identify and assign them correctly. In here we are interested in the hyperfine interaction caused by the ^{14}N nucleus (nuclear spin $J = 1$) of the NV center, which splits the $m_s = \pm 1$ ground state spin levels each into three hyperfine sublevels with an energy splitting of $\delta \approx 2.18\text{MHz}$. This energy splitting is seen in the CW electron spin resonance (ESR) measurement shown in Fig.2. In here, the ESR measurement is performed on the $m_s = 0 \rightarrow -1$ electron spin transition. Zero detuning corresponds to a driving microwave field of 2.4524GHz. Note, that a permanent magnetic field with a component along the NV axis of about 150G has been applied to shift the $m_s = 0 \rightarrow -1$ transition away from its zero field value (2.88GHz) owing to the Zeeman effect, and thus to separate it from the $m_s = 0 \rightarrow +1$ spin transition (which is shifted to higher frequency of 3.3GHz). This separation between the two electron spin transitions is necessary in order to ensure that the strong microwave field does not simultaneously drive both spin manifolds.

We now consider the Rabi beats expected for the given hyperfine splitting. For a driving microwave field that is detuned by a small frequency δ from the resonant tran-

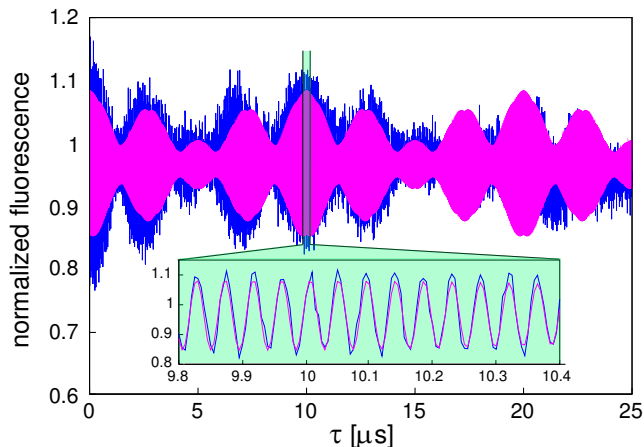


FIG. 3. Electron spin Rabi oscillations. Solid blue line: experimental data, solid magenta line: result from Fourier transform (Fig.4). Three beating cosine with frequencies corresponding to the three local maxima in the FFT are plotted.

sition, the Rabi frequency Ω is increased as compared to the resonant Rabi frequency Ω_0 , following [15]

$$\Omega = \sqrt{\Omega_0^2 + \delta^2}. \quad (4)$$

For small detuning ($\delta \ll \Omega_0$), the shift of the Rabi frequency $\delta\Omega$ becomes

$$\delta\Omega = \frac{\delta^2}{2\Omega_0}. \quad (5)$$

Suppose the microwave frequency corresponds to the lowest hyperfine transition (as in the present experiments). In this case, the lowest hyperfine transition is driven with Rabi frequency Ω_0 , while the two other hyperfine transitions are driven with faster Rabi frequencies corresponding to detunings $\delta_0 = 2.18\text{MHz}$ and $\delta_{-1} = 4.36\text{MHz}$. Using Eq. we can evaluate the expected Rabi frequencies. The resulting signal is the sum of three oscillations, whose frequencies can be extracted by Fourier transformation. Also, the three frequencies result in several beat frequencies in the Rabi signal.

To measure Rabi beats, a coplanar waveguide (gap= $10\mu\text{s}$, width= $10\mu\text{s}$) was fabricated directly onto a type IIa diamond sample with $\langle 100 \rangle$ crystallographic orientation and less than 4ppb nitrogen concentration (element6, electronic grade). A DC magnetic field was applied with a permanent magnet. A microwave field resonant to the lowest of the hyperfine transitions (2.4524GHz) was generated with a synthesizer (Rhode&Schwarz SMIQ) and applied to the sample through a fast switch (minicircuits ZASW-2-50DR). A single NV center was identified in the coplanar gap using a home built confocal fluorescence microscope. Rabi oscillations were measured using a standard laser- and microwave pulse sequence [7]. Figure 3 shows the corresponding Rabi oscillations. The data shows a base

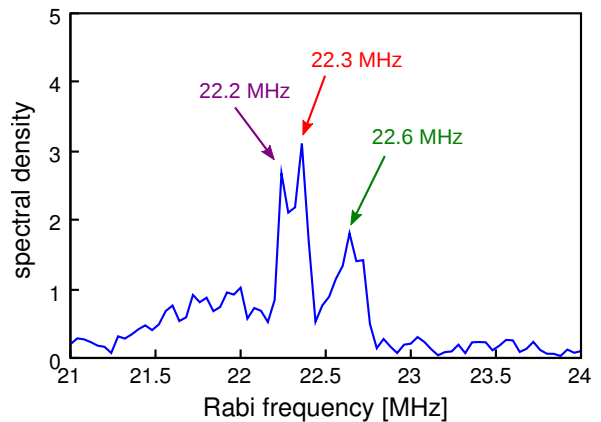


FIG. 4. Fourier transform of the Rabi signal. The data shows three distinct Rabi frequencies corresponding to the individual hyperfine levels.

oscillation of about 42MHz (see inset). Due to the beating this is approximately twice the base Rabi frequency. The two beat frequencies $\delta\Omega_0 = 100\text{kHz}$ and $\delta\Omega_{+1} = 400\text{kHz}$ correspond to the $m_s = 0$ and $m_s = +1$ hyperfine transition. Thus in total three Rabi oscillations are observed. Their individual frequencies are seen in the Fourier transform (Figure 4), that shows $\Omega_{-1} = 22.2\text{MHz}$, $\Omega_0 = 22.3\text{MHz}$, and $\Omega_{+1} = 22.6\text{MHz}$. Note that the FFT data is less pronounced due to the relatively sparse sampling of less than 10 points per period (see also zoom in Fig. 3) and power drift during the measurement. The sparse sampling was necessary to keep the total measurement time (several days for Fig. 3) within reasonable bounds. To complete our measurement of the hyperfine splitting from the Rabi beats, we use Eq. and convert the measured beats into energy level shifts. We find $\delta_0 = 2.1\text{MHz}$ and $\delta_{-1} = 4.2\text{MHz}$, which is in good agreement with the ESR spectrum (Fig.2).

The Rabi oscillations show a decay $T_1^* \approx 25\mu\text{s}$. This decay is much smaller than the expected $T_1^p \approx 1\text{ms}$ and is limited by microwave power drift as we show below. With the present decay T_1^* , the resolution of the hyperfine measurement is as follows. The resolution of a hyperfine measurement from the Rabi beats is determined by the Rabi frequency and the number N of visible Rabi oscillations. To measure a small change in the Rabi period, we need to measure a number of oscillations. Combining Eq.(5) with Eq.(4), we have

$$\delta = \frac{\Omega}{\sqrt{N}} = \frac{2\pi}{\sqrt{TT_1^*}}. \quad (6)$$

In our case we find $\delta \approx 6\text{MHz}$, which is in good qualitative agreement with our observations, since our data, in particular the Fourier transform, Fig.4, implies that we can indeed resolve the 4.32MHz detuning related to the farther detuned hyperfine level (22.6MHz peak in the FFT), however, we can just barely resolve the 2.16MHz

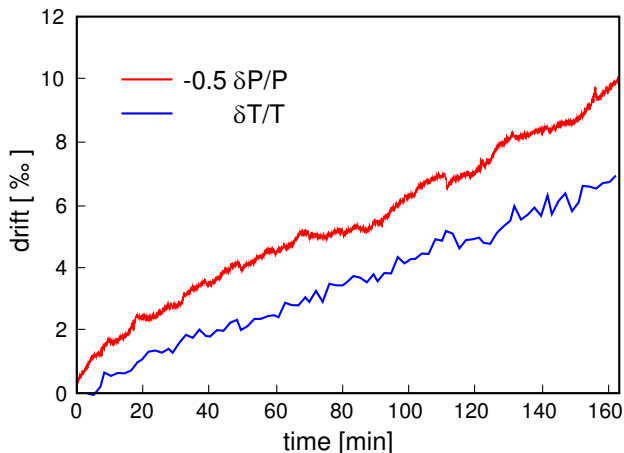


FIG. 5. Power drift. The relative change of the Rabi period is compared to the relative change of the microwave power.

detuning related to the lesser detuned hyperfine level (22.3MHz peak in the FFT). In the present measurements the total number of Rabi oscillations is about 500, which translates into an equivalent spatial resolution of about 10nm. We expect that an improvement of the power stability to a level better than 10^{-4} should be achievable without a large technical effort, and that spatial drifts of the microwave field should still be negligible in this case. Thus a spatial resolution of about 1nm should be achievable in a realistic measurement.

Any fluctuation or drift of the applied microwave power result in a small shift of the Rabi frequency over time, that washes out the oscillations. To proof that the observed decay is caused by power drift, we monitor the power transmitted through the sample and compare it to the Rabi period. This measurement is realized by successively performing short Rabi measurements in a small window ranging from $25.0\mu s$ to $25.1\mu s$. The result is shown in Figure 5. Since the Rabi period is inversely proportional to the frequency and the frequency is proportional to the square root of the power, we can express the relation between the relative change of the Rabi period as

$$\frac{\delta T}{T} = -\frac{1}{2} \frac{\delta P}{P}. \quad (7)$$

The data confirms that the decay time of the Rabi oscillations is limited by drift of the microwave power, which is slightly better than 10^{-3} over 24h in our case. Note that we also observed a change of the transmitted microwave power when the microscope objective was moved (about $10^{-3}/\mu m$). This is explained by a change of the parasitic capacitance of the coplanar waveguide, which plays a role owing to the close proximity of the high N.A. microscope objective to the sample (working distance $200\mu m$).

With the fast Rabi frequency required for a high spatial resolution, it is no longer feasible to shift the $m_s = \pm 1$ spin levels sufficiently far apart from each other such that

a single spin transitions is driven selectively. This is because the separation between the $m_s = \pm 1$ levels needed to be larger than the Rabi frequency. This would in turn require a large magnetic field. However at large magnetic field, level mixing causes the optical ESR contrast to vanish, unless the magnetic field is aligned parallel to the NV axis [10]. Alignment of the magnetic field parallel to the NV axis is however not possible in a sample with many randomly distributed NV centers. Thus, in a high resolution measurement, we will always measure with a small DC bias field and hence we will simultaneously drive the $m_s = \pm 1$ spin transitions. In this case, six hyperfine levels are present whose Rabi oscillations beat with each other. This situation differs from the previous experiments. While in the previous case, the Rabi signal was an incoherent sum of three oscillations (during a measurement, the nuclear spin switched randomly and slowly between the different spin states), now each nuclear spin manifold forms a V-type energy level scheme that is driven simultaneously. In the following, we evaluate the corresponding Rabi beat signal.

The NV's spin Hamiltonian with external magnetic field reads

$$H = \mathbf{H}_{ZFS} + \mathbf{H}_Z \quad (8)$$

with

$$\mathbf{H}_{ZFS} = D(\mathbf{S}_z^2 - \frac{2}{3}) + E(\mathbf{S}_x^2 - \mathbf{S}_y^2) \quad (9)$$

$$\mathbf{H}_Z = g\beta B \mathbf{S}_z. \quad (10)$$

After transforming into the energy Eigenbasis where we name the $m_s = 0$ state as $|0\rangle$ and the two state that correspond to the $m_s = \pm 1$ states as $|1\rangle$ and $|2\rangle$. Now the semiclassical microwave field is applied

$$\mathbf{H}_{MW} = \lambda e^{i\omega t} \mathbf{S}_x. \quad (11)$$

here we assume, that both transitions have the same transition matrix elements, which breaks down with rising E . Now do the rotating wave approximation (RWA) and transform into the rotating frame which leaves us with a Hamiltonian of the form

$$\mathbf{H}_{rot} = \begin{pmatrix} 0 & \lambda & \lambda \\ \lambda & \Delta - \delta & 0 \\ \lambda & 0 & \Delta + \delta \end{pmatrix}. \quad (12)$$

where $\delta = \Delta E_{|1\rangle|2\rangle}/2$ and Δ the detuning of the microwave from $|1\rangle + \delta$.

To obtain an analytical solution we set $\Delta = 0$. Calculation of the Eigenvalues leads to the Rabi frequency $\sqrt{2V^2 + \delta^2}$ which, were the two levels detuned is $\sqrt{2}$ times the Rabi frequency of driving a single level. We now take a look at the time evolution of the system with initial state $|0\rangle$. The dynamics of $|0\rangle$ are

$$\rho_{|0\rangle} = \frac{(\delta^2 + 2\lambda^2 \cos[\sqrt{2\lambda^2 + \delta^2} t])^2}{(2\lambda^2 + \delta^2)^2}. \quad (13)$$

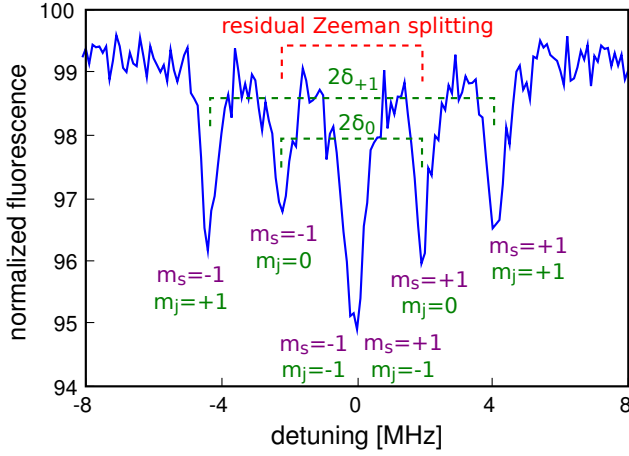


FIG. 6. ESR spectrum of the second NV center without DC bias field. The two hyperfine triplets corresponding to the $m_s = -1$ and $m_s = +1$ spin levels overlap in the central dip. Detuning is denoted relative to the central hyperfine transition corresponding to 2.8706GHz.

from here we see, that there are actually two oscillation frequencies involved, the Rabi frequency and double the Rabi frequency corresponding to the \cos^2 term. The latter will be the base Rabi frequency observed in experiments, and we find the identity for the Rabi beat as

$$\delta\Omega = \frac{2\delta^2}{\Omega_0}, \quad (14)$$

which is different from the previous expression, Eq.(.).

To measure Rabi beats with V-type microwave excitation, we remove the DC bias field. Moreover we pick a different NV center that is closer to the central conductor and feels a higher microwave power. Figure 6 shows the ESR spectrum, with a total of five dips. The central dip is about twice larger as compare to the other dips. In this experiment, the Zeeman splitting due to a residual magnetic field (earth magnetic field as well as magnetized parts of the setup) closely matches the hyperfine splitting. As a consequence, the two hyperfine triplets corresponding to the $m_s = -1$ and $m_s = +1$ spin transition are shifted in such a way that the highest peak of the lower triplet overlaps with the lowest peak of the higher triplet, resulting in five dips with a pronounced central dip. Rabi oscillations are now driven with the microwave frequency tuned in resonance with the central dip corresponding to 2.8706GHz. This case corresponds to the theoretical case $\Delta = 0$ treated above, with $\delta_0 = 2.18$ MHz and $\delta_{+1} = 4.36$ MHz for the driving of the $m_j = 0$ and $m_j = +1$ manifold, respectively.

The Rabi oscillations and their Fourier transform are shown in Figure 7 and 8. The first observation is that the Rabi frequency is increased by about a factor of two as compared to the previous case. Two effects contribute here. First, with lambda type driving the Rabi frequency

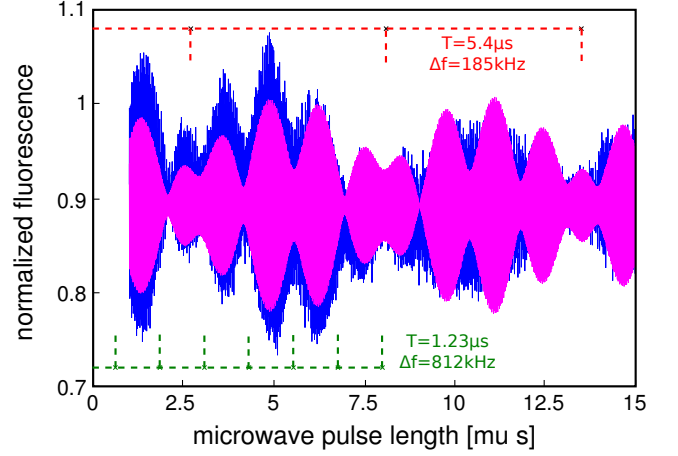


FIG. 7. Rabi oscillations under V-type microwave excitation. Solid blue line: experimental data. Red and green markers denote the extracted beat frequencies. Solid magenta line: result of the extracted beat frequencies. Three beating cosine with the corresponding frequency shifts are plotted.

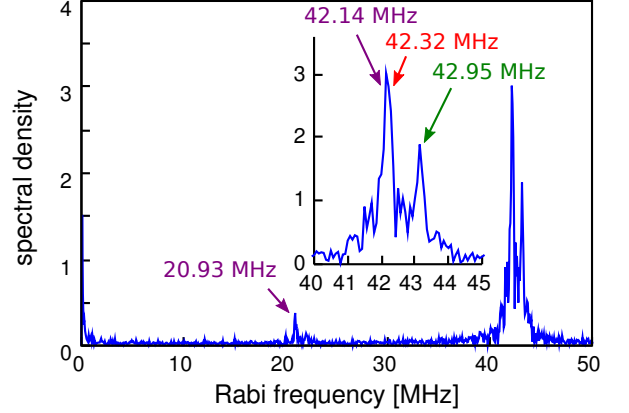


FIG. 8. Fourier transform of the Rabi oscillations under V-type microwave excitation. Peaks around 42MHz and 21MHz correspond to the base Rabi oscillations and a modulation at half the frequency. The inset shows the beating Rabi frequencies around 42MHz. Labels mark the three frequencies as extracted from the beat analysis of the raw data. The FFT resolves the fast beat, while it does not resolve the slow beat due to sparse sampling.

is enhanced by a factor of $\sqrt{2}$ as compared to driving a single transition, and second, the Rabi frequency is additionally increased due to the higher microwave power in the close vicinity of the central conductor. The second observation is a fast and a slow beat with frequency of about 185kHz and 812kHz, respectively. These beats are seen most clearly in the Rabi oscillations. Note that the slower beat is not resolved in the FFT (Fig.8) due to power drift and sparse sampling. We can now convert the observed beatings to energy level shifts according to Eq.(.). We find $\delta_0 = 2.0$ MHz and $\delta_{+1} = 4.1$ MHz, which

is in good agreement with the ESR spectrum.

SUMMARY AND CONCLUSIONS

We have performed two proof-of-principle experiments towards T_1 limited magnetic resonance imaging with NV centers in diamond. First, we have demonstrated the measurement of a large number (> 500) of Rabi flops, and we have shown that the hyperfine interaction due to ^{14}N can be resolved from such a measurement. Second, we have studied the Rabi beats without a large DC bias field, where the nuclear spin manifolds form V-type energy level schemes. The base Rabi frequency is increased by $\sqrt{2}$ and the time evolution of the state population is modulated by an oscillation with half the base Rabi frequency. While the present experiments were performed in bulk, in the future, it will be an important step to demonstrate Rabi beat imaging with NV centers embedded in diamond nano crystals. The present experiments are relevant to quantum information processing in diamond. The ability to drive a large number of Rabi flops could allow to precisely control the spin state of several (detuned) NV centers simultaneously. We envision a microwave pulse with precisely adjusted length that performs independent unitary transformations on a quantum register, such as rotate an NV A to $|1\rangle$ while simultaneously rotating an NV B to the superposition $\sqrt{2}(|0\rangle + |1\rangle)$.

ACKNOWLEDGEMENTS

This work was supported by the European Union, Deutsche Forschungsgemeinschaft (SFB/TR21 and FOR1482), Bundesministerium für Bildung und Forschung, and the Landesstiftung Badenwürttemberg.

* helmut.fedder@gmail.com

- [1] G. Balasubramanian, IY Chan, R. Kolesov, M. Al-Hmoud, J. Tisler, C. Shin, C. Kim, A. Wojcik, P.R. Hemmer, A. Krueger, et al. Nanoscale imaging magnetometry with diamond spins under ambient conditions. *Nature*, 455(7213):648–651, 2008.
- [2] G. Balasubramanian, P. Neumann, D. Twitchen, M. Markham, R. Kolesov, N. Mizuochi, J. Isoya, J. Achard, J. Beck, J. Tissler, et al. Ultralong spin coherence time in isotopically engineered diamond. *Nature Materials*, 8(5):383–387, 2009.
- [3] Eric Betzig, George H. Patterson, Rachid Sougrat, O. Wolf Lindwasser, Scott Olenych, Juan S. Bonifacio, Michael W. Davidson, Jennifer Lippincott-Schwartz, and Harald F. Hess. Imaging Intracellular Fluorescent Proteins at Nanometer Resolution. *Science*, 313(5793):1642–1645, 2006.
- [4] I. Chiorescu, Y. Nakamura, C. Harmans, and JE Mooij. Coherent quantum dynamics of a superconducting flux qubit. *Science*, 299(5614):1869, 2003.
- [5] G. de Lange, D. Ristè, VV Dobrovitski, R. Hanson, M. Sciacca, X. Hong, SH Cheng, C. Herding, J. Zhu, M. Kormos, et al. Single-spin magnetometry with multipulse dynamical decoupling sequences. *Arxiv preprint arXiv:1008.4395*, 2010.
- [6] S.W. Hell and J. Wichmann. Breaking the diffraction resolution limit by stimulated emission: stimulated-emission-depletion fluorescence microscopy. *Optics Letters*, 19(11):780–782, 1994.
- [7] F. Jelezko, T. Gaebel, I. Popa, A. Gruber, and J. Wrachtrup. Observation of coherent oscillations in a single electron spin. *Physical review letters*, 92(7):76401, 2004.
- [8] JR Maze, PL Stanwix, JS Hodges, S. Hong, JM Taylor, P. Cappellaro, L. Jiang, M.V.G. Dutt, E. Togan, AS Zibrov, et al. Nanoscale magnetic sensing with an individual electronic spin in diamond. *Nature*, 455(7213):644–647, 2008.
- [9] S. Meiboom and D. Gill. Modified spin-echo method for measuring nuclear relaxation times. *Review of Scientific Instruments*, 29:688, 1958.
- [10] P. Neumann, J. Beck, M. Steiner, F. Rempp, H. Fedder, P.R. Hemmer, J. Wrachtrup, and F. Jelezko. Single-Shot Readout of a Single Nuclear Spin. *Science*, 329(5991):542, 2010.
- [11] A. Pertsinidis, Y. Zhang, and S. Chu. Subnanometre single-molecule localization, registration and distance measurements. *Nature*, 466(7306):647–651, 2010.
- [12] DA Redman, S. Brown, RH Sands, and SC Rand. Spin dynamics and electronic states of NV centers in diamond by EPR and four-wave-mixing spectroscopy. *Physical review letters*, 67(24):3420–3423, 1991.
- [13] M.J. Rust, M. Bates, and X. Zhuang. Sub-diffraction-limit imaging by stochastic optical reconstruction microscopy (STORM). *Nature Methods*, 3(10):793–796, 2006.
- [14] Arthur Schweiger and Gunnar Jeschke. *Principles of pulsed electron paramagnetic resonance*. University Press, Oxford, 2001.
- [15] Marlan O. Scully and M. Suhail Zubairy. *Quantum Optics*. Cambridge University Press, 3 edition, 1999.
- [16] C. Shin, C. Kim, R. Kolesov, G. Balasubramanian, F. Jelezko, J. Wrachtrup, and P.R. Hemmer. Sub-optical resolution of single spins using magnetic resonance imaging at room temperature in diamond. *Journal of Luminescence*, 2009.
- [17] J. Tisler, G. Balasubramanian, B. Naydenov, R. Kolesov, B. Grotz, R. Reuter, J.P. Boudou, P.A. Curmi, M. Senour, A. Thorel, et al. Fluorescence and spin properties of defects in single digit nanodiamonds. *ACS Nano*, 3(7):1959–1965, 2009.